

Received: 2017.12.30
Accepted: 2018.01.12
Published: 2018.08.13

Micro-RNA-137 Inhibits Tau Hyperphosphorylation in Alzheimer's Disease and Targets the *CACNA1C* Gene in Transgenic Mice and Human Neuroblastoma SH-SY5Y Cells

Authors' Contribution:
Study Design A
Data Collection B
Statistical Analysis C
Data Interpretation D
Manuscript Preparation E
Literature Search F
Funds Collection G

ABCE 1,2 **Yang Jiang**
BDE 2 **Bing Xu**
BDE 3 **Jing Chen**
ABCDF 1,2 **Yi Sui**
BF 2 **Li Ren**
BD 1 **Jing Li**
CD 1 **Huiyu Zhang**
DF 1 **Liqing Guo**
AG 1 **Xiaohong Sun**

1 Department of Neurology, The Fourth Affiliated Hospital of China Medical University, Shenyang, Liaoning, P.R. China
2 Department of Neurology and Neuroscience, Shenyang First People's Hospital, Shenyang Brain Hospital, Shenyang Brain Institute, Shenyang, Liaoning, P.R. China
3 Department of Neurology and Neuroscience, Shenyang Tenth People's Hospital, Shenyang Chest Hospital, Shenyang, Liaoning, P.R. China

Corresponding Author: Xiaohong Sun, e-mail: xhsun@cmu.edu.cn

Source of support: This study was supported by grants from the National Natural Science Foundation of China (No. 81371395), the Natural Science Foundation of Liaoning Province (No. 20170541021 and No. 2015020547), and the China Post-doctoral Science Foundation (No. 2015MS81375)

Background: Alzheimer's disease (AD) results in cognitive impairment. The calcium voltage-gated channel subunit alpha-1 C *CACNA1C* gene encodes an alpha-1 C subunit of L-type calcium channel (LTCC). The aim of this study was to investigate the role of micro-RNA-137 (miR-137) and the *CACNA1C* gene in APPswe/PS1ΔE9 (APP/PS1) double-transgenic AD mice and in human neuroblastoma SH-SY5Y cells.


Material/Methods: Six-month-old APP/PS1 double-transgenic AD mice (N=6) and age-matched normal C57BL/6 mice (N=6) underwent a Morris water maze (MWM) test, expression levels of amyloid-β (Aβ), LTCC, the *CACNA1C* gene, and miR-137 were measured in the rat hippocampus and cerebral cortex in both groups of mice. A luciferase assay was used to evaluate the effect of miR-137 on the expression of *CACNA1C* in SH-SY5Y human neuroblastoma SH-SY5Y cells. Western blotting was used to detect the *CACNA1C*, phosphorylated-tau (p-tau), and Aβ proteins.

Results: In APP/PS1 transgenic AD mice, spatial learning and memory was significantly reduced, levels of Aβ₁₋₄₀ and Aβ₁₋₄₂ were increased in the serum, hippocampus, and cerebral cortex, expression levels of miR-137 were reduced, expression of *CACNA1C* protein was increased in the hippocampus and cerebral cortex, compared with normal control mice. miR-137 regulated the expression of the *CACNA1C* gene. Increased expression levels of p-tau (Ser202, Ser396, and Ser404) induced by Aβ₁₋₄₂ were inhibited by miR-137 mimics in SH-SY5Y human neuroblastoma cells *in vitro*.

Conclusions: In a transgenic mouse model of AD, miR-137 and expression of the *CACNA1C* gene inhibited the hyperphosphorylation of tau protein.

MeSH Keywords: 14-3-3 Proteins • Alzheimer Disease • Amyloid beta-Peptides • MicroRNAs

Full-text PDF: <https://www.medscimonit.com/abstract/index/idArt/908765>

 3374

 1

 5

 36



Background

Alzheimer's disease (AD) is a neurodegenerative disease, characterized by memory loss, cognitive impairment, and intellectual impairment [1]. Worldwide, the prevalence of AD is increasing, and it has been estimated that AD will affect more than 35 million people by 2050 [2]. Currently, AD is the most common neurodegenerative disease in humans and results in a very large and increasing economic and clinical burden on modern society [3]. The cerebral pathology of AD is marked by the neurofibrillary amyloid plaques and abnormal protein deposits, composed of amyloid- β ($A\beta$) peptides ($A\beta_{1-40}$ and $A\beta_{1-42}$) and the accumulation of intracellular insoluble hyperphosphorylated tau proteins (p-tau). Several previously published studies have shown that AD begins in the areas of the brain that are associated with learning and memory, and then spreads to the hippocampus, temporal cortex, frontoparietal cortex, and finally to the subcortical nuclei [4,5]. Currently, there are no diagnostic biomarkers for the early detection of AD, and there are no effective drug treatments that delay or prevent the progression of AD. Therefore, further studies are required to identify AD-related genes and to develop screening methods for these genes to improve the diagnosis and the therapy for AD.

Recent studies have shown that micro-RNAs (miRNAs) are involved in the pathogenesis of AD [6], and that miRNAs might play important roles in neurogenesis, neuronal maturation, and brain development [7,8], and might regulate several neurodegenerative diseases, including AD [9,10]. Several miRNAs, including miR-206 and miR-219, have been shown to be associated with the pathogenesis of AD [11,12], and micro-RNA-137 (miR-137) is a brain-enriched miRNA, has been shown to be associated with neurodegenerative diseases, including as schizophrenia [11], and AD [12]. Also, increased activity of L-type calcium (Ca^{2+}) channels (LTCCs) has also been implicated in the pathogenesis of AD [13–15]. LTCCs consist of an $\alpha 1$ subunit ($CaV1.1$, -1.2 , -1.3 , or -1.4), an accessory $\alpha 2\Delta$ as well as β subunits [16]. In these subunits, the $\alpha 1$ subunits not only contain the channel pore and the voltage-sensor but also determine the pharmacological properties, while the accessory subunits regulate membrane expression and gating properties of the calcium channels. Two types of LTCCs, $CaV1.2$ and $CaV1.3$, are mainly expressing in the mammalian brain [17,18]. These voltage-gated calcium channels mediate calcium entry into the neurons and regulate multiple neuronal cell functions, such as synaptic plasticity, excitability, and transcriptional regulation. Association analysis has shown that miR-137 and its potential target gene *CACNA1C* (calcium voltage-gated channel subunit alpha-1 C) are reported to be associated with both schizophrenia and bipolar disorder [11]. However, data is still lacking on the roles of miR-137 and *CACNA1C* in the pathogenesis of AD [12].

The aim of this study was to investigate the role of miR-137 and the *CACNA1C* gene in APPswe/PS1 Δ E9 (APP/PS1) double-transgenic AD mice and in human neuroblastoma SH-SY5Y cells. The study was designed to investigate the effect of miR-137 in the pathogenesis of AD both in the AD mouse model *in vivo* and in the SH-SY5Y cell line *in vitro*. The expression levels of amyloid- β ($A\beta$) peptides including $A\beta_{1-40}$ and $A\beta_{1-42}$, and levels of miR-137 with its potential target gene, *CACNA1C*, both in the mouse hippocampus and cerebral cortex were compared between the AD mouse model and healthy control mice. The study was also designed to investigate the regulatory effect of miR-137 on the transcription of its potential target gene, *CACNA1C*, and on the phosphorylation levels of tau proteins in SH-SY5Y cells.

Material and Methods

Ethical statement

All animal experiments were performed in strict accordance with the Institutional Animal Care and Use Committee (IACUC) and approved by China Medical University Animal Care and Use Committee.

Animals

Six-month-old male APPswe/PS1 Δ E9 (APP/PS1) double-transgenic Alzheimer's disease (AD) mice (N=6) (18–22 gm) and age-matched normal C57BL/6 mice (N=6) (18–22 gm) were purchased from Nanjing Biomedical Research Institute of Nanjing University (Nanjing, China).

Morris water maze (MWM) test

A Morris water maze (MWM), 120 cm in diameter, and 40 cm in height, with a water depth of 24 cm was purchased from Anhui Zhenghua Biological Instrument Equipment Company (Anhui, China). The MWM test was performed to detect spatial learning and memory ability between the healthy control mice (N=6) and AD mice (N=6). The MWM apparatus was split into four quadrants with a platform, 9 cm in diameter and 23 cm in height, which was placed in the third quadrant. The MWM test consisted of two components, a place navigation test from day 1 to day 5, and a spatial probe test on day 6. During the place navigation test, four contiguous trials were performed each day. Each mouse was allowed an adaptation period of 20 seconds on the platform, then placed in each quadrant respectively, and given 60 seconds to reach the platform. The mice that reached the platform within 60 seconds remained on the platform for 5 seconds, while the mice were manually guided to the platform if the mice could not reach the platform within 60 seconds and remained on the platform for 10

Table 1. Primer list for real-time PCR.

Primer name	Sequence (5'-3')
miR-137-3p F	GGACACGCTTATTGCTTAAGAATA
miR-137-3p R	GTGCAGGGTCCGAGGTATTC
U6-F	CTCGCTTCGGCAGCAC
U6-R	AACGCTTCACGAATTTGCGT

seconds. During the spatial probe test, the platform was removed and the mice were placed in the first quadrant. The escape latency, swimming path, and target zone frequency of the mice were recorded.

Total RNA extraction, cDNA synthesis, and quantitative real-time polymerase chain reaction (qRT-PCR)

Total RNA was extracted using a high purity total RNA extraction kit (BioTeke, Beijing, China) and cDNAs were synthesized from RNA templates by Super M-MLV reverse transcriptase (BioTeke, Beijing, China). The reverse transcription products were then amplified using the SYBR Green reaction mix (SolarBio, Beijing, China). The primers used are shown in Table 1.

The reaction conditions of reverse transcription were as follows: 25°C for 10 min, 42°C for 50 min, and 80°C 5 min. The PCR amplification conditions were: 95°C for 10 min, 40 cycles of 95°C for 10 seconds, 60°C for 20 seconds and 72°C for 30 seconds, and then 4°C for 5 min. The PCR reaction was performed on Exicycler™ 96 Real-Time Quantitative Thermal Block (Bioneer, Daejeon, Korea). Quantitative real-time polymerase chain reaction (qRT-PCR) was performed four times. Data was determined via the $2^{-\Delta\Delta CT}$ method [19].

Western blot analysis

The tissue and cell samples were collected and lysed with RIPA buffer (Beyotime, Beijing, China) containing 1% phenylmethylsulphonyl fluoride (PMSF) (Beyotime, Beijing, China). The protein concentration was measured by BCA Protein Assay Kit (Beyotime, Beijing, China). Primary antibodies for calcium voltage-gated channel subunit alpha-1 C (*CACNA1C*) (1: 200) (Santa Cruz, Santa Cruz, CA, USA), phosphorylated-tau (p-tau) (Ser 202) (1: 400) (Boster, Wuhan, China), p-tau (Ser 396) (1: 5000) (Abcam, Cambridge, MA, USA), p-tau (Ser 404) (1: 500) (Sangon, Shanghai, China), tau (1: 500) (Sangon, China) and amyloid- β ($A\beta$) (1: 1000) (Sigma, St. Louis, USA) were used in this study.

Equal amounts of protein samples were separated on a 10% sodium dodecyl sulfate-polyacrylamide gel electrophoresis (SDS-PAGE) gel and transferred onto a polyvinylidene difluoride (PVDF) membrane (Millipore, Bedford, MA, USA). The

membrane was blocked with 5% dried skimmed milk powder and incubated with primary antibodies and horseradish peroxidase (HRP)-labeled goat anti-rabbit IgG (H+L) secondary antibody (1: 5000) (Beyotime, Beijing, China). Proteins were visualized by ECL Reagent (Seven Sea Biotech, Shanghai, China) and imaged with a gel imaging system. β -actin was used as an internal control.

Enzyme-linked immunosorbent assay (ELISA)

The levels of amyloid- β ($A\beta$) peptides $A\beta_{1-40}$ and $A\beta_{1-42}$ were measured by ELISA using an ELISA Kit for $A\beta_{1-40}$ and $A\beta_{1-42}$ (USCN, Wuhan, China) following the manufacturer's instructions. The values at 450 nm were read using a microplate reader (BioTek, Winooski, VT, USA).

Immunofluorescence (IF) assay

Sections of mouse cerebral cortex and hippocampus were fixed in formalin and embedded in paraffin wax. Tissue sections were cut at 5- μ m onto glass slides, and sections were dewaxed with xylene and rehydrated with alcohol. Tissue sections underwent microwave antigen-retrieval for 10 min and blocked with goat serum (ZSGB-BIO, Beijing, China). The sections were incubated with primary antibodies for *CACNA1C* protein and $A\beta$ overnight at 4°C, washed and then incubated with fluorescein isothiocyanate (FITC)-labeled goat anti-mouse IgG (H+L) and Cy3-labeled goat anti-rabbit IgG (H+L) secondary antibodies. Cell nuclear staining was done with 4',6-diamidino-2-phenylindole (DAPI) (Beyotime, Beijing, China).

Cell culture

Human SH-SY5Y neuroblastoma cells were cultured in Dulbecco's modified Eagle's medium (DMEM) (Gibco, MA, USA) containing 10% heat-inactivated fetal bovine serum (FBS) (Hyclone Co., Logan, USA), 100 units/ml of penicillin/streptomycin (Gibco®, Grand Island, USA) in 37°C in a humidified atmosphere of 5% CO₂. $A\beta_{1-42}$ (5 μ M) was purchased from GL Biochem (Shanghai, China). Cells were firstly transfected with or without miR-137 mimics, miR-137 inhibitors, or normal control (NC) miRNA and treated for 48 hours. Then, the cultured cells were stimulated with 5 μ M $A\beta_{1-42}$ for 24 hours, and the cells were collected for the later experiments.

Cell transfection and luciferase assay

Luciferase assays were measured using the Dual-Luciferase® Reporter (DLR™) Assay System (Promega, Madison, WI, USA) according to the manufacturer's instructions. A 424-bp DNA fragment of the human *CACNA1C* gene containing the binding region of miR-137 was first amplified by using the following primer pair:

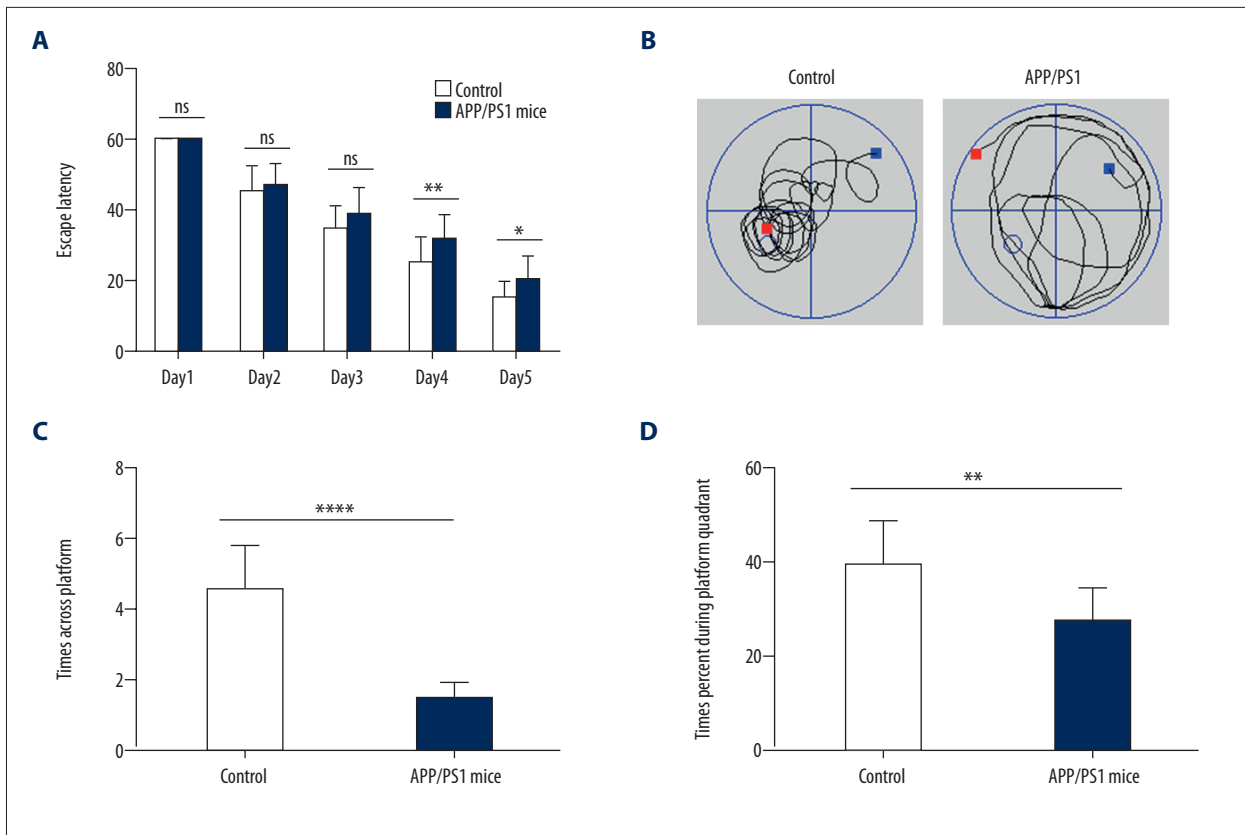


Figure 1. Behavioral evaluation of the APPswe/PS1 Δ E9 (APP/PS1) double-transgenic mouse Alzheimer's disease (AD) model by the Morris water maze (MWM) test. **(A)** The mean daily latencies of escape in the normal C57BL/6 control mice (N=6) and the APPswe/PS1 Δ E9 (APP/PS1) double-transgenic Alzheimer's disease (AD) mouse model (N=6). **(B)** Representative tracks for the AD mouse model and the normal C57BL/6 control mice in the Morris water maze (MWM) test at day 6. **(C, D)** The times across the platform and percentage of time in each platform quadrant, at day 6 of the MWM. The comparison is between the two groups, the AD mouse model and the normal C57BL/6 control mice. Statistically significant differences between groups are denoted by * $P < 0.05$, ** $P < 0.01$, *** $P < 0.001$, **** $P < 0.0001$.

forward, 5'-CTAGCTAGCGGTTGTCTGTGTGC-3', and reverse, 5'-ACTCGTCGACCTGAAACTGACCTGA-3'. For the mutant type, the seed sequence was mutated as follows: forward, 5'-CAATGCTTAAATATTCATTTAAAAA-3', and reverse, 5'-ATATTTAAGCATTGTTTTGCATAT-3'.

These fragments were then inserted into pmirGLO vectors between NheI and Sall. The co-transfection of pmirGLO plasmids and miRNA mimics in SH-SY5Y cells was performed by using Lipofectamine 2000 reagent (Invitrogen, Grand Island, NY, USA) according to the manufacturer's instructions. Forty-eight hours later, the Renilla luciferase activity was measured. The ratio of firefly to Renilla luciferase of each sample was calculated in triplicate.

Statistical analysis

Statistical analysis was performed using GraphPad 6.0. Differences between two groups were determined using

one-way analysis of variance (ANOVA), and multiple comparisons were performed with a Bonferroni *post hoc* test. Data were presented as the mean \pm standard deviation (SD). $P < 0.05$ was considered to be statistically significant.

Results

Behavioral evaluation and amyloid- β (A β) production between the APP/PS1 transgenic Alzheimer's disease (AD) model mice and the C57BL/6 healthy control mice

To compare the behavioral differences between the APPswe/PS1 Δ E9 (APP/PS1) double-transgenic Alzheimer's disease (AD) model mice and C57BL/6 healthy control mice, the Morris water maze (MWM) test was performed. The escape latency to reach the platform in AD mice was significantly longer compared with the C57BL/6 healthy control mice at day 4 and day 5 (Figure 1A) ($P < 0.05$). Representative swimming paths are shown

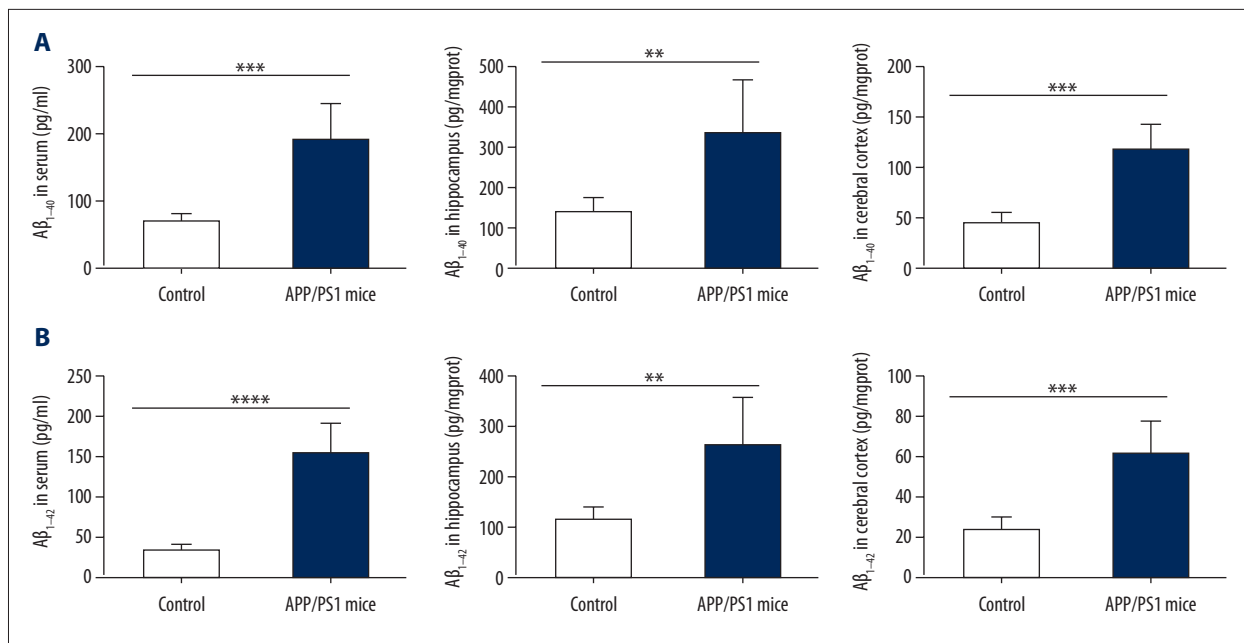


Figure 2. Levels of amyloid- β ($A\beta$) peptides, $A\beta_{1-40}$ and $A\beta_{1-42}$ in the mouse serum, hippocampus, and cerebral cortex in the APPswe/PS1 Δ E9 (APP/PS1) double-transgenic Alzheimer's disease (AD) mice and the normal C57BL/6 control mice, measured by enzyme-linked immunosorbent assay (ELISA). **(A, B)** Levels of the $A\beta_{1-42}$ amyloid- β ($A\beta$) peptides $A\beta_{1-40}$ **(A)** and $A\beta_{1-42}$ **(B)** in the normal C57BL/6 control mice (N=6) and the APPswe/PS1 Δ E9 (APP/PS1) double-transgenic Alzheimer's disease (AD) mice (N=6) are measured by an enzyme-linked immunosorbent assay (ELISA). Differences between groups are denoted by * $P < 0.05$, ** $P < 0.01$, *** $P < 0.001$, **** $P < 0.0001$.

in Figure 1B. AD mice crossed less frequently within the platform area compared with the C57BL/6 healthy control mice (Figure 1B). Also, the spatial probe test showed that the number of times the mice crossed the platform and the percentage of time in the target quadrant in the AD mice group were significantly reduced when compared with the C57BL/6 healthy control mice (Figure 1C, 1D) ($P < 0.01$). Expression levels of phosphorylated-tau (p-tau) (Ser202, Ser396, and Ser404) induced by $A\beta_{1-42}$ amyloid- β ($A\beta$) peptides $A\beta_{1-40}$ and $A\beta_{1-42}$ in serum, hippocampus, and cerebral cortex between the AD mice and C57BL/6 healthy control mice were tested by enzyme-linked immunosorbent assay (ELISA) (Figure 2). The AD model mice had increased levels of $A\beta_{1-40}$ and $A\beta_{1-42}$ in serum, hippocampus, and cerebral cortex compared with the C57BL/6 healthy control mice (Figure 2A, 2B) ($P < 0.01$). Therefore, the AD model mice showed significantly impaired learning and memory ability compared with the C57BL/6 healthy control mice.

The expression levels of miR-137 were reduced and the expression levels of *CACNA1C* were increased in the APP/PS1 transgenic Alzheimer's disease (AD) model mice compared with these levels in the C57BL/6 healthy control mice

To study the role of miR-137 in AD mice, the levels of miR-137 in the hippocampus and cerebral cortex in both the AD mice

and C57BL/6 healthy control mice were also detected by real-time polymerase chain reaction (qRT-PCR) analysis. Data showed that levels of miR-137 in the hippocampus and cerebral cortex of AD mice were lower compared with the control mice (Figure 3A) ($P < 0.01$). Because calcium voltage-gated channel subunit alpha-1 C (*CACNA1C*) was also implicated in the pathogenesis of AD, the protein level of *CACNA1C* was also measured by Western blot. The protein level of *CACNA1C* in both the hippocampus and cerebral cortex of AD mice was significantly increased compared with the control mice (Figure 3B). Also, double immunofluorescence staining of *CACNA1C* and $A\beta$ was seen in both the hippocampus and cerebral cortex of AD mice (Figure 3C). These findings indicated that the level of miR-137 was decreased, whereas the level of *CACNA1C* was increased in the hippocampus and cerebral cortex of AD mice compared with healthy control mice.

MiR-137 regulated *CACNA1C* gene expression in human neuroblastoma SH-SY5Y cells

To identify the direct target of miR-137 in mediating the pathological course of AD, bioinformatics analysis was performed and predicted that *CACNA1C* gene transcript was a candidate target of miR-137. The 3'-UTR of the *CACNA1C* transcript contains putative miR-137 binding sites (Figure 4A), and the luciferase reporter assay was performed to verify their interaction.

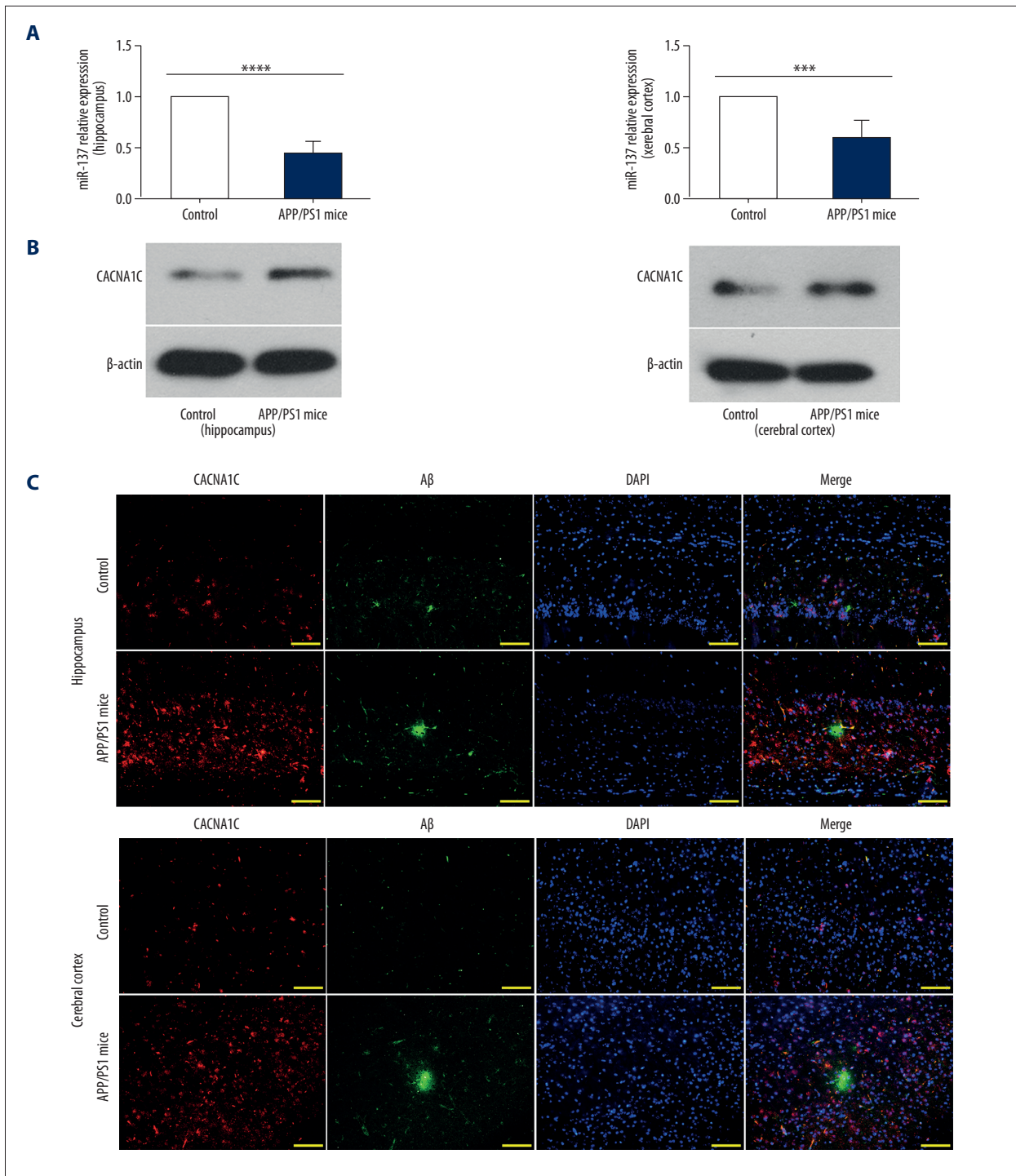


Figure 3. Expression levels of micro-RNA-137 (miR-137), the *CACNA1C* protein, and amyloid- β ($A\beta$) in the normal C57BL/6 control mice (N=6) and the APP^{swe}/PS1 Δ E9 (APP/PS1) double-transgenic Alzheimer's disease (AD) mice (N=6). **(A)** The expression levels of micro-RNA-137 (miR-137) in the hippocampus and cerebral cortex of healthy control mice (N=6) and the APP/PS1 Alzheimer's disease (AD) mice are measured by quantitative real-time polymerase chain reaction (qRT-PCR) analysis. **(B)** Western blot shows that the protein level of calcium voltage-gated channel subunit alpha-1 (*CACNA1C*) is increased in the APP/PS1 AD mice. **(C)** The immunofluorescence (IF) assay shows increased expression levels of *CACNA1C* protein and amyloid- β ($A\beta$)-containing plaques in both the hippocampus and cerebral cortex in APP/PS1 AD mice compared with healthy controls. Scale bar, 100 μ m.

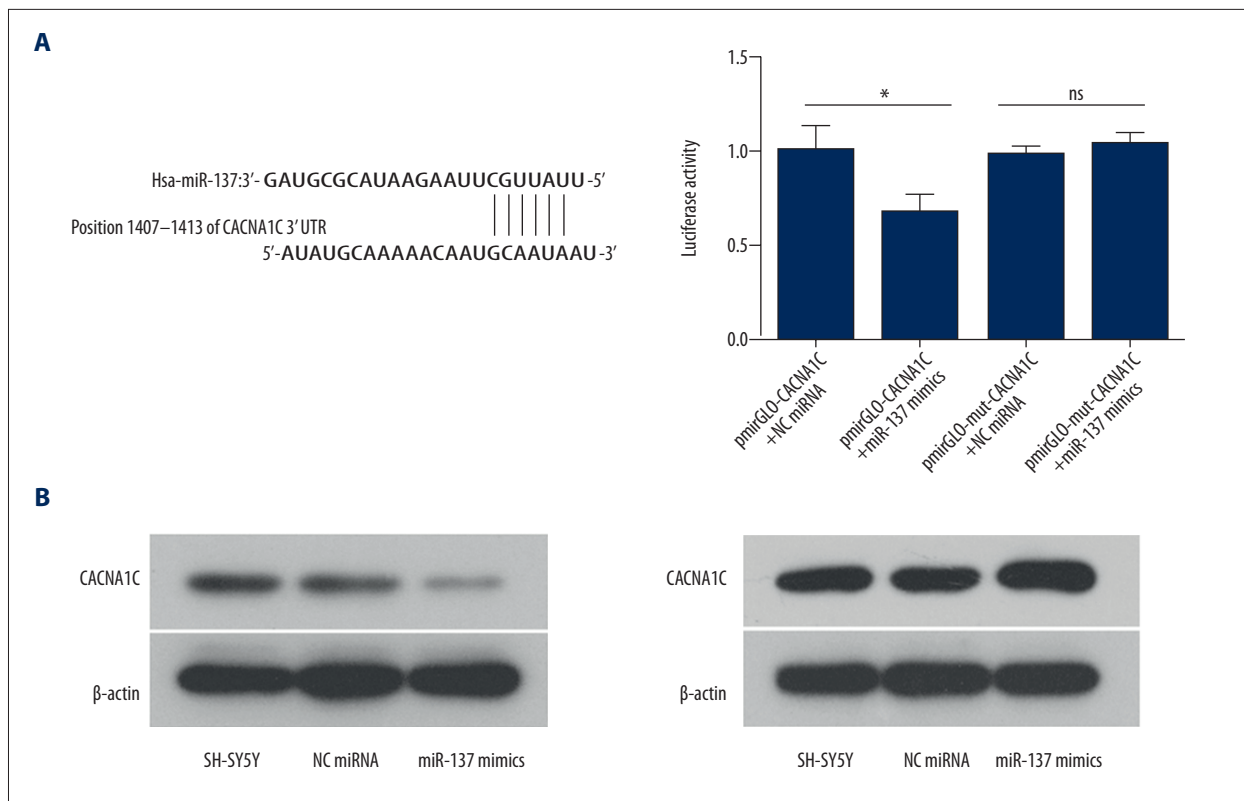


Figure 4. micro-RNA-137 (miR-137) targets the *CACNA1C* gene in human neuroblastoma SH-SY5Y cells. **(A) (left panel).** The predicted micro-RNA-137 (miR-137) binding sites on the 3'-UTR of *CACNA1C* transcript (from TargetScanHuman, Version 7.1, June 2016). **(A) (right panel).** Luciferase reporter assay on the interaction between miR-137 and *CACNA1C* 3'-UTR. A mutant *CACNA1C* (mut-*CACNA1C*) is tested to validate the specific binding. **(B)** The regulatory effects of miR-137 on the expression of *CACNA1C* in human neuroblastoma SH-SY5Y cells. The expression levels of *CACNA1C* protein measured by Western blot analysis. Statistically significant differences between groups are denoted by * $P < 0.05$.

Figure 4B shows the significant inhibitory effect of miR-137 on the activity of luciferase reporter for *CACNA1C* 3'-UTR but not mut-*CACNA1C* 3'-UTR (Figure 4B) ($P < 0.01$). The regulatory role of miR-137 in *CACNA1C* expression was further validated by examining *CACNA1C* expression in human neuroblastoma SH-SY5Y cells transfected with miR-137 mimics or inhibitors, by Western blot analysis. Data showed that compared with SH-SY5Y cells transfected with NC-miRNA, miR-137 mimics significantly decreased the protein expression level of *CACNA1C*, whereas miR-137 inhibitor increased the *CACNA1C* level in SH-SY5Y cells (Figure 4B). Therefore, miR-137 inhibited the expression of *CACNA1C* by directly binding to the 3'-UTR of *CACNA1C* mRNA in SH-SY5Y cells.

miR-137 suppressed the phosphorylation of tau induced by $A\beta_{1-42}$ in SH-SY5Y cells

To evaluate the possible regulatory effect of miR-137 on $A\beta_{1-42}$ -induced hyperphosphorylation of tau, SH-SY5Y cells transfected with miR-137 mimics, miR-137 inhibitor, or NC-miRNA were treated with or without $A\beta_{1-42}$. The results indicated treatment

with $A\beta_{1-42}$ significantly increased the levels of hyperphosphorylation of tau at the sites Ser202, Ser396 and Ser404 in SH-SY5Y cells. However, this increased hyperphosphorylation of tau was significantly inhibited by miR-137 mimics, whereas transfection with miR-137 inhibitor increased $A\beta_{1-42}$ -induced hyperphosphorylation of tau in SH-SY5Y cells (Figure 5). These results indicate that miR-137 suppressed the $A\beta_{1-42}$ -induced hyperphosphorylation of tau in SH-SY5Y cells.

Discussion

Alzheimer's disease (AD) is characterized by the accumulation of intracellular accumulation of insoluble hyperphosphorylated tau proteins (p-tau) and abnormal protein deposits, or plaques, composed of amyloid- β ($A\beta$) peptides ($A\beta_{1-40}$ and $A\beta_{1-42}$). Although extensive research has been dedicated to the identification the pathogenesis and prevention of AD, these processes remain poorly understood.

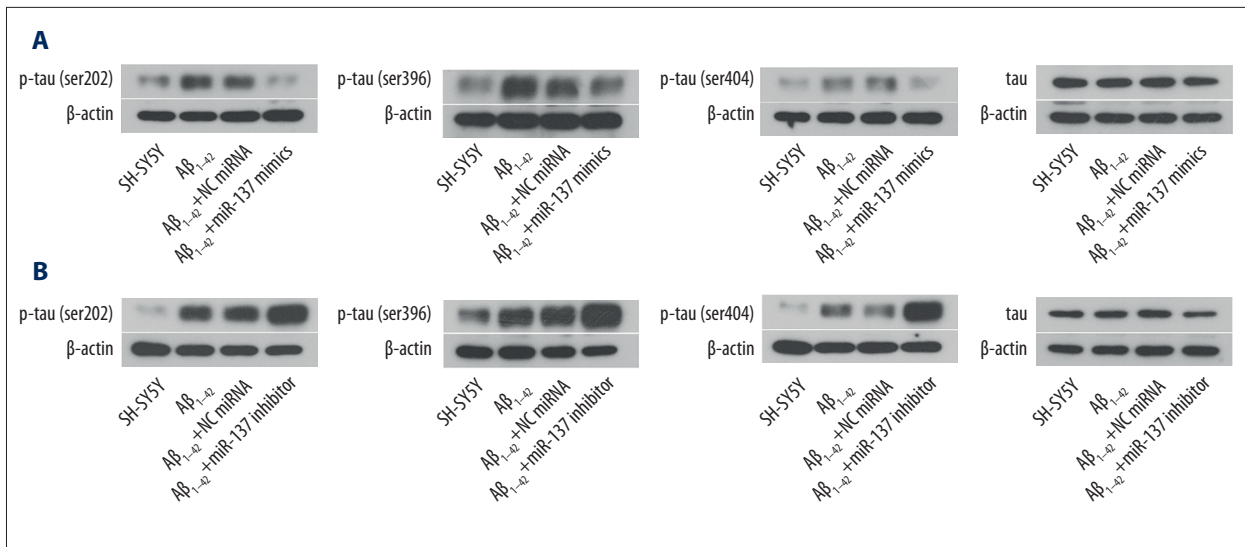


Figure 5. micro-RNA-137 (miR-137) suppresses the phosphorylation of tau protein (p-tau) in human neuroblastoma SH-SY5Y cells. (A, B) The levels of p-tau (ser202), p-tau (ser396), p-tau (ser404) and tau protein in amyloid- β ($A\beta$) peptide $A\beta_{1-42}$ -induced human neuroblastoma SH-SY5Y cells transfected with micro-RNA-137 (miR-137) mimics or miR-137 inhibitors are analyzed by Western blot.

Micro-RNAs (miRNAs) have been shown to be potential biomarkers and therapeutic targets for a variety of psycho-neurologic disorders [20]. micro-RNA-137 (miR-137) has been shown to be a regulator of neuronal development and cognitive function, was identified as a predictor for a cognitively impaired subtype of schizophrenia and reduced positive psychosis symptoms of schizophrenia [21,22] [38], and as a regulator for $A\beta$ expression in AD patients [23]. However, studies on the functions of miR-137 in AD remain limited. In the present study, the regulation and function of miR-137 in an APPsw/PS1 Δ E9 (APP/PS1) double-transgenic mouse model of AD was investigated *in vivo* and in human neuroblastoma SH-SY5Y cells *in vitro*, with the aim of the study being to determine the role of miR-137 and the *CACNA1C* gene in AD mice and in human neuroblastoma SH-SY5Y cells.

The findings of this study were that spatial learning and memory ability in the APP/PS1 transgenic mice, which were utilized as an AD model, were significantly decreased compared with the C57BL/6 healthy control mice using the Morris water maze (MWM) test. Also, levels of $A\beta_{1-40}$ and $A\beta_{1-42}$, key proteins associated with the pathogenesis of AD, were increased in the serum, hippocampus, and cerebral cortex in AD mice, compared with healthy controls. The level of miR-137 was decreased, whereas the protein expression of *CACNA1C* was increased both in the hippocampus and cerebral cortex of AD mice. Data from this study showed that miR-137 regulated the expression of *CACNA1C* by binding to the 3' UTR of its mRNA, with the increased expression levels of phosphorylated tau (p-tau) (Ser202, Ser396, and Ser404) induced by $A\beta_{1-42}$ inhibited by miR-137 mimics in the human neuroblastoma SH-SY5Y cells.

miR-137 levels have been shown clinically to be decreased in the serum of patients with AD and could be used as a marker for early diagnosis [24]. Loss of miR-137 and miR-181c has been shown to increase serine palmitoyltransferase (SPT), which is the first rate-limiting enzyme that elevates ceramide levels, which have been reported to be associated with sporadic AD, and the generation of $A\beta$, which is a protein that contributes to the pathogenesis of AD when located in the brain [12]. In the present study, a decrease in miR-137 levels and an increase in $A\beta$ levels in the AD mouse hippocampus and cerebral cortex were observed. miR-137 has been reported to regulate certain forms of schizophrenia by binding to its target genes *CSMD1*, *C10orf26*, *TCF4*, and also *CACNA1C* [25]. Until now, *CACNA1C* expression was regarded as a risk factor for multiple neuropsychiatric disorders, such as bipolar disorder and depressive disorders, as determined by molecular analysis [26,27]. The up-regulation of *CACNA1C* caused by $A\beta$ peptides has also been previously shown to be associated with AD risk *in vitro* [28]. The data from the present study showed that when accompanied by an increasing level of $A\beta$, the *CACNA1C* gene was up-regulated in the hippocampus and cerebral cortex in AD mice and that miR-137 regulated the expression of the *CACNA1C* gene by binding to *CACNA1C* 3'UTR directly in SH-SY5Y cells.

Previously published studies have shown that hyperphosphorylation of tau is highly correlated with the neurodegeneration in AD, which leads to reduced ability to bind microtubules, resulting in a destabilization of microtubule network, and neurofibrillary tangle formation [29], as well as neuronal death [30]. Tau has been confirmed to be phosphorylated at more than 30 serine/threonine residues in the brains of AD patients [31].

The results of the present study showed that SH-SY5Y cells exposed to $A\beta_{1-42}$ could induce hyperphosphorylation of tau at Ser202, Ser396, and Ser404, which was inhibited by miR-137 in this study. Previously published studies have reported that several kinases, including p-38, MAPK, ERK, and GSK3 β have been shown to regulate the phosphorylation of tau [32,33]. Jakobsson et al. found that the hyperphosphorylated tau: total tau ratio in cerebrospinal fluid of patients with bipolar disorder was significantly associated with the single nucleotide polymorphism (SNP) rs1006737, situated in *CACNA1C* encoding the alpha 1C subunit of the L-type voltage-gated calcium channel CaV1.2 [34]. Cav1.2 is clustered at postsynaptic sites [35], where it contributes to calcium influx; an increase in calcium influx through CaV1.2 is thought to contribute to neuronal dysfunctions such as is found in AD [13]. Furukawa et al. have previously reported that tau mutation interacts with L-type calcium channel activity in SH-SY5Y cells [36]. From the findings of the above studies, together with the findings of the present study, it may be possible to propose that miR-137 inhibits $A\beta$ -induced hyperphosphorylation of tau by targeting *CACNA1C* in AD disease.

This study had several limitations, and was a preliminary study that included small numbers of study mice (AD model) and control mice. The findings of the study showed that miR-137 inhibited the hyperphosphorylation of tau and directly targeted

the 3'UTR of *CACNA1C* in the SH-SY5Y cells *in vitro*. However, the relative interactions between miR-137, p-tau, *CACNA1C*, and $A\beta$, and the regulatory effect of miR-137 on the progression of AD *in vivo* require further investigation.

Conclusions

The findings of this study, using a double-transgenic mouse model of Alzheimer's disease (AD) and human neuroblastoma SH-SY5Y cells, have shown that expression levels of microRNA-137 (miR-137) were low in AD mice, which might indicate the regulatory function of miR-137 in the pathogenesis of AD by inhibiting the hyperphosphorylation of the tau protein. Also, miR-137 regulated the expression of the calcium voltage-gated channel subunit alpha-1 C (*CACNA1C*) gene by directly binding to the 3'-UTR of *CACNA1C* in SH-SY5Y cells. The findings of this study have shown a novel interaction between miR-137 and *CACNA1C*, which suggests that miR-137 may be a potential diagnostic or therapeutic target for AD. Further studies are recommended to investigate the role of miR-137 in AD.

Conflict of interest

None.

References:

1. Alzheimer's Association: 2014 Alzheimer's disease facts and figures. *Alzheimers Dement*, 2014; 10: e47-92
2. Danborg PB, Simonsen AH, Waldemar G, Heegaard NH: The potential of microRNAs as biofluid markers of neurodegenerative diseases: A systematic review. *Biomarkers*, 2014; 19: 259-68
3. Querfurth HW, Laferla FM: Alzheimer's disease. *N Engl J Med*, 2010; 362: 329-44
4. Reddy PH, Manczak M, Mao P et al: Amyloid-beta and mitochondria in aging and Alzheimer's disease: Implications for synaptic damage and cognitive decline. *J Alzheimers Dis*, 2010; 20(Suppl. 2): S499-512
5. Reddy PH, Mcweeney S: Mapping cellular transcriptomes in autopsied Alzheimer's disease subjects and relevant animal models. *Neurobiol Aging*, 2006; 27: 1060-77
6. Reddy PH, Tonk S, Kumar S et al: A critical evaluation of neuroprotective and neurodegenerative MicroRNAs in Alzheimer's disease. *Biochem Biophys Res Commun*, 2017; 483: 1156-65
7. Saba R, Schrott GM: MicroRNAs in neuronal development, function and dysfunction. *Brain Res*, 2010; 1338: 3-13
8. Kapsimali M, Kloosterman WP, De Bruijn E et al: MicroRNAs show a wide diversity of expression profiles in the developing and mature central nervous system. *Genome Biol*, 2007; 8: R173
9. Kumar S, Reddy PH: Are circulating microRNAs peripheral biomarkers for Alzheimer's disease? *Biochim Biophys Acta*, 2016; 1862: 1617-27
10. Long JM, Lahiri DK: Current drug targets for modulating Alzheimer's amyloid precursor protein: Role of specific micro-RNA species. *Curr Med Chem*, 2011; 18: 3314-21
11. Guan F, Zhang B, Yan T et al: MIR137 gene and target gene *CACNA1C* of miR-137 contribute to schizophrenia susceptibility in Han Chinese. *Schizophr Res*, 2014; 152: 97-104
12. Geekiyanage H, Chan C: MicroRNA-137/181c regulates serine palmitoyltransferase and in turn amyloid beta, novel targets in sporadic Alzheimer's disease. *J Neurosci*, 2011; 31: 14820-30
13. Davare MA, Hell JW: Increased phosphorylation of the neuronal L-type Ca(2+) channel Ca(v)1.2 during aging. *Proc Natl Acad Sci USA*, 2003; 100: 16018-23
14. Daschil N, Obermair GJ, Flucher BE et al: CaV1.2 calcium channel expression in reactive astrocytes is associated with the formation of amyloid-beta plaques in an Alzheimer's disease mouse model. *J Alzheimers Dis*, 2013; 37: 439-51
15. Min D, Guo F, Zhu S et al: The alterations of Ca2+/calmodulin/CaMKII/CaV1.2 signaling in experimental models of Alzheimer's disease and vascular dementia. *Neurosci Lett*, 2013; 538: 60-65
16. Catterall WA: Structure and regulation of voltage-gated Ca2+ channels. *Annu Rev Cell Dev Biol*, 2000; 16: 521-55
17. Striessnig J, Koschak A, Sinnegger-Brauns MJ et al: Role of voltage-gated L-type Ca2+ channel isoforms for brain function. *Biochem Soc Trans*, 2006; 34: 903-9
18. Sinnegger-Brauns MJ, Huber IG, Koschak A et al: Expression and 1,4-dihydropyridine-binding properties of brain L-type calcium channel isoforms. *Mol Pharmacol*, 2009; 75: 407-14
19. Livak KJ, Schmittgen TD: Analysis of relative gene expression data using real-time quantitative PCR and the 2(-Delta Delta C(T)) method. *Methods*, 2001; 25: 402-8
20. O'Connor RM, Gururajan A, Dinan TG et al: All roads lead to the miRNome: miRNAs have a central role in the molecular pathophysiology of psychiatric disorders. *Trends Pharmacol Sci*, 2016; 37: 1029-44
21. Olde Loohuis NF, Nadif Kasri N, Glennon JC et al: The schizophrenia risk gene MIR137 acts as a hippocampal gene network node orchestrating the expression of genes relevant to nervous system development and function. *Prog Neuropsychopharmacol Biol Psychiatry*, 2017; 73: 109-18

22. Cummings E, Donohoe G, Hargreaves A et al: Mood congruent psychotic symptoms and specific cognitive deficits in carriers of the novel schizophrenia risk variant at MIR-137. *Neurosci Lett*, 2013; 532: 33–38
23. Geekiyanage H, Chan C: SPT, miR-137 and miR-181c: Therapeutic targets and noninvasive biomarkers. *Alzheimers Dementia*, 2012; 8: P470–P1
24. Geekiyanage H, Jicha GA, Nelson PT, Chan C: Blood serum miRNA: Non-invasive biomarkers for Alzheimer's disease. *Exp Neurol*, 2012; 235: 491–96
25. Kwon E, Wang W, Tsai LH: Validation of schizophrenia-associated genes CSMD1, C10orf26, CACNA1C and TCF4 as miR-137 targets. *Mol Psychiatry*, 2013; 18: 11–12
26. Green EK, Grozeva D, Jones I et al: The bipolar disorder risk allele at CACNA1C also confers risk of recurrent major depression and of schizophrenia. *Mol Psychiatry*, 2010; 15: 1016–22
27. Rao S, Yao Y, Zheng C et al: Common variants in CACNA1C and MDD susceptibility: A comprehensive meta-analysis. *Am J Med Genet B Neuropsychiatr Genet*, 2016; 171: 896–903
28. Anekonda TS, Quinn JF, Harris C et al: L-type voltage-gated calcium channel blockade with isradipine as a therapeutic strategy for Alzheimer's disease. *Neurobiol Dis*, 2011; 41: 62–70
29. Leszek J, Malyszczak K, Janicka B et al: Total tau in cerebrospinal fluid differentiates Alzheimer's disease from vascular dementia. *Med Sci Monit*, 2003; 9: CR484–88
30. Medina M, Avila J: New perspectives on the role of tau in Alzheimer's disease. Implications for therapy. *Biochem Pharmacol*, 2014; 88: 540–47
31. Martin L, Latypova X, Wilson CM et al: Tau protein kinases: Involvement in Alzheimer's disease. *Ageing Res Rev*, 2013; 12: 289–309
32. Perry G, Roder H, Nunomura A et al: Activation of neuronal extracellular receptor kinase (ERK) in Alzheimer disease links oxidative stress to abnormal phosphorylation. *Neuroreport*, 1999; 10: 2411–15
33. Zhu X, Rottkamp CA, Boux H et al: Activation of p38 kinase links tau phosphorylation, oxidative stress, and cell cycle-related events in Alzheimer disease. *J Neuropathol Exp Neurol*, 2000; 59: 880–88
34. Jakobsson J, Palsson E, Sellgren C et al: CACNA1C polymorphism and altered phosphorylation of tau in bipolar disorder. *Br J Psychiatry*, 2016; 208: 195–96
35. Davare MA, Avdonin V, Hall DD et al: A beta2 adrenergic receptor signaling complex assembled with the Ca2+ channel Cav1.2. *Science*, 2001; 293: 98–101
36. Furukawa K, Wang Y, Yao PJ et al: Alteration in calcium channel properties is responsible for the neurotoxic action of a familial frontotemporal dementia tau mutation. *J Neurochem*, 2003; 87: 427–36